References and Notes

1. G. J. Wasserburg and D. A. Papanastassiou, *Earth Planet. Sci. Lett.* **13**, 97 (1971); D. A. Papanastassiou and G. J. Wasserburg, *ibid.* **13**, 368 (1972).
2. F. Tera, D. A. Papanastassiou, G. J. Wasserburg, in *Lunar Science—IV, Houston, March 1973*, J. W. Chamberlain and C. Watkins, Eds. (Lunar Science Institute, Houston, 1973), p. 723; D. A. Papanastassiou and G. J. Wasserburg, *Earth Planet. Sci. Lett.* **16**, 289 (1972).
3. L. Husain and D. A. Schaeffer, in *Lunar Science—IV, Houston, March 1973*, J. W. Chamberlain and C. Watkins, Eds. (Lunar Science Institute, Houston, 1973), p. 406.
4. F. El-Baz, A. M. Worden, V. D. Brand, *Geochim. Cosmochim. Acta* (Suppl. 3), 85 (1972).
5. F. El-Baz, *ibid.*, p. 39; E. W. Wolfe, V. L. Freeman, W. R. Muehlberger, J. W. Head, H. H. Schmitt, J. W. Sevier, *Geotimes* **17**, 14 (1973).
6. Apollo Field Geology Investigation Team, *Science* **182**, 672 (1973).
7. Lunar Sample Preliminary Examination Team, *ibid.* **165**, 1211 (1969).
8. Apollo 16 Preliminary Examination Team, *ibid.* **179**, 23 (1973).
9. Apollo 15 Preliminary Examination Team, *ibid.* **175**, 363 (1972).
10. D. S. McKay, G. H. Heiken, R. M. Taylor, U. S. Clanton, D. A. Morrison, G. H. Ladle, *Geochim. Cosmochim. Acta* (Suppl. 3) 983 (1972).
11. D. S. McKay, D. A. Morrison, U. S. Clanton, G. H. Ladle, J. F. Lindsay, *ibid.* (Suppl. 2) 755 (1971).
12. A. M. Reid, G. E. Lofgren, G. H. Heiken, R. W. Brown, G. Moreland, *EOS* **6**, 606 (1973).
13. J. L. Warner, *Geochim. Cosmochim. Acta* (Suppl. 3) 623 (1972).
14. A. M. Reid, J. L. Warner, W. I. Ridley, R. W. Brown, *Meteoritics* **7**, 395 (1972).
15. A. M. Reid, W. I. Ridley, R. S. Harmon, J. L. Warner, R. Brett, P. Jakes, R. W. Brown, *Geochim. Cosmochim. Acta* **36**, 903 (1972).
16. G. Cavarretta, R. Funiciello, H. Giles, G. D. Nicholls, A. Taddeucci, J. Zussman, *The Apollo 15 Lunar Samples* (Lunar Science Institute, Houston, 1972), p. 202.
17. G. W. Reed, personal communication.
18. L. Husain and O. A. Schaeffer, Verbal report at Apollo 17 Session, Fourth Lunar Science Conference, Houston, March 1973.
19. T. Kirsten, Verbal report at Apollo 17 Session, Fourth Lunar Science Conference, Houston, March 1973.
20. C. H. Simonds, J. L. Warner, W. C. Phinney, R. Gooley, *Lunar Science—IV, Houston, March 1973*, J. W. Chamberlain and C. Watkins, Eds. (Lunar Science Institute, Houston, 1973), p. 676; A. E. Bence, J. J. Papike, S. Sueno, J. W. Delano, *ibid.*, p. 60; A. L. Albee, A. J. Gancarz, A. A. Chodos, *ibid.*, p. 24.
21. N. J. Hubbard and P. W. Gast, *Geochim. Cosmochim. Acta* (Suppl. 2) 999 (1971); N. J. Hubbard, P. W. Gast, J. M. Rhodes, B. M. Bansal, H. Wiesmann, *ibid.* (Suppl. 3) 1161 (1972).
22. K. A. Howard and H. G. Wilshire, *Lunar Science—IV, Houston, March 1973*, J. W. Chamberlain and C. Watkins, Eds. (Lunar Science Institute, Houston, 1973), p. 389.
23. R. A. F. Grieve and A. G. Plant, *ibid.*, p. 317.
24. X-ray fluorescence analysis of rocks and soils was done by J. M. Rhodes, K. V. Rodgers, and B. M. Bansal.
25. N. J. Hubbard, P. W. Gast, J. M. Rhodes, B. M. Bansal, H. Wiesmann, *Geochim. Cosmochim. Acta* (Suppl. 3), 1161 (1972).

Geologic Exploration of Taurus-Littrow: Apollo 17 Landing Site

Apollo Field Geology Investigation Team

Apollo 17 landed in a deep graben valley embaying the mountainous highlands southeast of the Serenitatis basin. Impact-generated breccias underlie the massifs adjacent to the valley, and basalt has flooded and leveled the valley floor. The dark mantle inferred from orbital photographs was not recognized as a discrete unit; the unusually thick regolith of the valley floor contains a unique high concentration of dark glass beads that may cause the low albedo of much of the surface.

Apollo 17 landed at latitude 20°10′N and longitude 30°46′E on the flat floor of a deep, narrow valley that embays the mountainous highlands at the southeastern rim of the Serenitatis basin (Fig. 1). Serenitatis is one of the major multiringed basins on the near side of the moon and the site of a pronounced mascon (*1*). The Taurus-Littrow valley, which is radial to the Serenitatis basin, is interpreted as a deep graben formed initially by structural adjustment of lunar crustal material to the Serenitatis impact (*2, 3*).

During their stay on the lunar surface, astronauts E. A. Cernan and H. H. Schmitt traversed a total of about 30 kilometers, collected about 110 kilograms of rocks and soil, and took more than 2200 photographs. Their traverses, sampling, direct observations, and photographs spanned the full width of the Taurus-Littrow valley (Fig. 2).

The highlands surrounding the valley can be divided on the basis of morphology into two major units, high steep massifs with slopes of about 25° and smaller, closely spaced domical hills referred to as sculptured hills (Fig. 3). Both units were interpreted in pre-mission studies as deposits of ejecta derived from surrounding basins with major uplift occurring in the Serenitatis event. A possible volcanic origin was also considered but thought to be less likely (*2, 4*). An additional low hills unit adjacent to the massifs was considered to be downfaulted and partly buried blocks of massif or sculptured hills material (*4, 5*). Material from massifs north and south of the valley was obtained by sampling boulders that had rolled down their slopes. These boulders are composed of complex breccias that are generally similar to those returned on Apollo 15 and Apollo 16.

Materials of the valley fill were sampled at many stations. Ejecta around many craters on the valley floor consists of basalt, showing that the graben was partially filled by lava flows. A relatively thick layer of unconsolidated material overlies the subfloor basalt; it consists largely of finely comminuted rock debris.

The material at the surface over much of the Taurus-Littrow region has a very low albedo and was believed be-

This article is a condensation and revision of a report by the Apollo Field Geology Investigation Team to be included in the Apollo 17 Preliminary Science Report for the National Aeronautics and Space Administration. The condenser, E. W. Wolfe (U.S. Geological Survey, Flagstaff, Arizona), and the principal investigator for Apollo field geology investigations, W. R. Muehlberger (University of Texas, Austin, and USGS), assume full responsibility for any distortions of concepts or data developed by other authors of the original report. Direct contributions to the work reported here were made by W. R. Muehlberger; R. M. Batson (USGS); E. A. Cernan (National Aeronautics and Space Administration, Houston, Texas); V. L. Freeman, M. H. Haitt, H. E. Holt, K. A. Howard, E. D. Jackson, K. B. Larson, and V. S. Reed (USGS); J. J. Rennilson (California Institute of Technology, Pasadena); H. H. Schmitt (NASA); and D. H. Scott, R. L. Sutton, D. Stuart-Alexander, G. A. Swann, N. J. Trask, G. E. Ulrich, H. G. Wilshire, and E. W. Wolfe (USGS). Some of the concepts were developed in part in pre-mission discussions with J. W. Head (Brown University, Providence, Rhode Island) and B. K. Lucchitta (USGS). The quality of the manuscript was improved as a result of critical reviews by B. K. Lucchitta and J. P. Schafer (USGS).

fore the mission to be a thin young dark mantle, possibly pyroclastic, that covered the valley floor and parts of the adjacent highlands. No clear evidence of the existence of such a mantle as a discrete layered unit has yet been found, but it may be mixed with the more typical debris of the regolith.

An unusual bright deposit, called the light mantle, extends across the valley floor from the foot of South Massif. It consists of breccias similar to those of the massif and is interpreted as a landslide generated on the massif slopes.

Massif Materials, Sculptured Hills

Massif materials consist mainly of three major types of breccias that we class as light gray, blue-gray, and greenish-gray (*6, 7*). All three types were collected from each massif sampling station (stations 2, 6, and 7) as well as from the light mantle.

Light gray breccias are the most variable type. At station 2 and on the light mantle they contain abundant dark-gray fine-grained lithic clasts up to several millimeters across in a friable to moderately coherent light gray matrix. A small percentage of white clasts is contained within both the dark-gray clasts and the matrix. At stations 6 and 7, the light gray breccias consist of friable white or very light gray angular mineral debris. Some samples contain clasts of fine-grained blue-gray breccia.

Greenish-gray breccias are vesicular, vuggy, and annealed. They contain a small percentage of mineral and lithic clasts in a fine-grained sugary matrix. Vesicles range up to several millimeters in diameter. The vugs, which are commonly flattened and locally preferentially aligned, range from 0.1 to 9 centimeters in diameter; the largest occur in the station 6 boulder. Lithic clasts, generally less than 10 mm across, include (i) fine-grained pale gray hornfels, (ii) cataclastically deformed rock rich in plagioclase, and (iii) granoblastic intergrowths of plagioclase and a yellow-green silicate mineral.

Blue-gray breccias consist of 10 percent or less lithic and mineral clasts in a tough, deep bluish-gray matrix that is dense, fine-grained to aphanitic, and holocrystalline. Lithic clasts are largely cataclastic and sugary white rocks with hornfels texture. At station 2, where blue-gray breccia forms the matrix of one boulder, local concentrations of slit-like cavities are elongated parallel to a weak alignment of lithic clasts. Blue-gray breccia in the station 6 boulder actually consists of a high proportion (40 to 60 percent) of blue-gray breccia fragments in a vuggy greenish-gray matrix. Vugs that are 2 to 5 mm across and lined with brown pyroxene and plagioclase occur in both the matrix and the blue-gray breccia clasts.

At South Massif, samples were collected from three breccia boulders (Fig. 4), two of which may have rolled down from a blue-gray unit and the underlying tan unit recognized by the crew near the top of the massif. The sampled boulders are about 50 meters above the break in slope at the base of the massif (station 2 of Fig. 2) in a field of boulders directly below a blocky area that may represent outcrops high on the slope. As no other sources of boulders are visible lower on the slope, the blocky area is the probable source of the sampled boulders.

One sampled boulder, about 2 m across by 1 m high, is a foliated layered breccia, the only one of its type seen by the astronauts. Their observations suggest that it represents the blue-gray unit at the top of the massif. Four samples collected from it all consist of light gray breccia.

The second sampled boulder from South Massif is a fractured rock about 2 m in diameter from which five samples of vuggy, greenish-gray breccia were collected. Two of the samples were taken from a 0.5-m clast, and the remaining three samples were taken from the matrix of the boulder. The two clast samples are somewhat lighter in color than two of the matrix samples, but closely resemble the third. The boulder may have come from the tan unit high on the massif.

The third boulder is an equant, subangular breccia boulder about 40 cm across. Two samples, one of the boulder matrix and the other of a breccia clast, were collected. The matrix sample is a blue-gray vesicular breccia, the clast a light greenish-gray breccia.

Additional South Massif materials were collected from the light mantle at stations 2a and 3 (Fig. 2). These include samples of light gray breccia, blue-gray breccia, and greenish-gray breccia that are all similar to the samples from the station 2 boulders.

Materials of North Massif were sampled primarily from a large (6 by 10 by 18 m) fragmented boulder at station 6 (Fig. 5), and a 3-m boulder at sta-

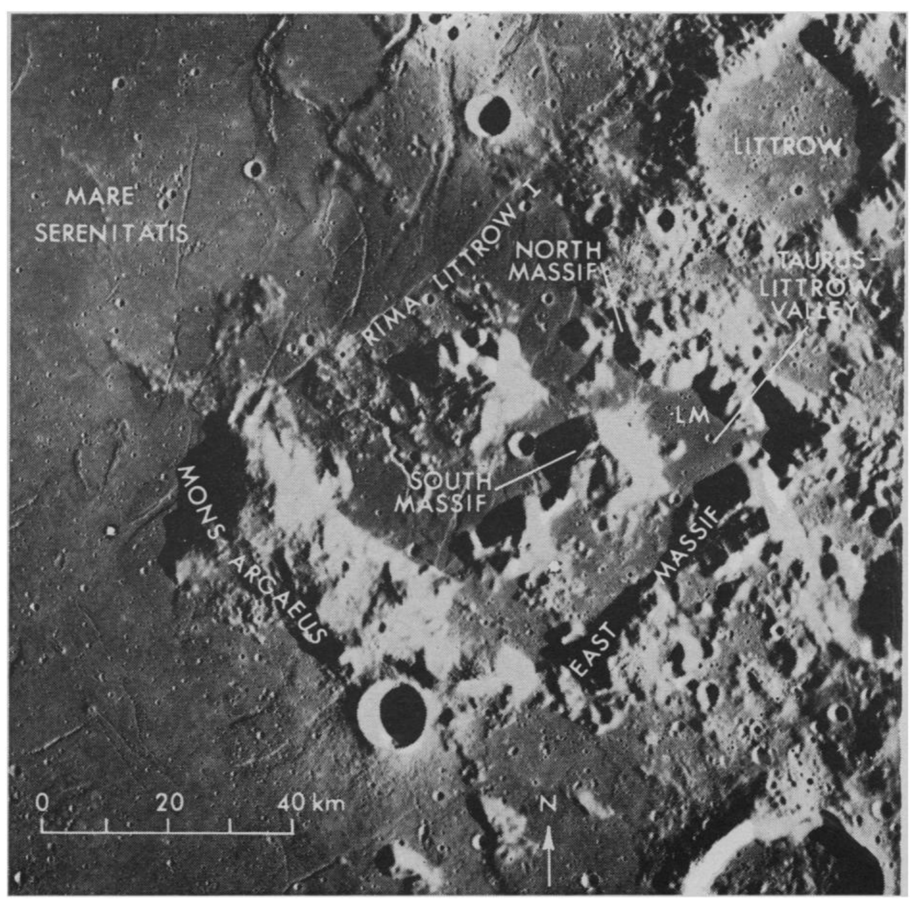

Fig. 1. Index map showing the Apollo 17 landing site and major geographic features of the Taurus-Littrow region. [NASA mapping camera photograph AS17-M-447]

tion 7. The station 6 boulder is at the lower end of a boulder track whose apparent beginning is in an area of light boulders about one-third of the way up the massif (Fig. 6). Dark boulders are abundant higher on the mountain, and light boulders occur again in its upper part. Thus there may be a layer or lenses of darker rock high on the mountain, with lighter rocks both above and below. The source of the station 7 boulder on North Massif is unknown, but it contains rock types like those of the station 6 boulder.

The station 6 boulder is in five pieces, the largest of which is about 10 m across. The original boulder can be pieced back together, generally with only a small amount of rotation of any of the blocks (Fig. 5b). Several large fragments that may have broken from the boulder as it rolled downhill can be seen in and near the boulder track.

Samples were collected from boulder fragments 1, 2, 4, and 5 (Fig. 5b). The boulder consists of two major breccia types: (i) blue-gray breccia in fragments 1 and 2, and (ii) greenish-gray breccia in fragments 2, 3, 4, and 5. An irregular contact between the two breccia types occurs in fragment 2. The contact zone, approximately 50 cm across, appears to be an area of mixing between the two rock types.

Within the blue-gray breccia of fragment 1 there are white friable inclusions ranging in size from 1 or 2 cm to 1 m across which are in sharp, irregular contact with the blue-gray breccia. Chips representing one of these inclusions are very light gray cataclasites.

The station 6 boulder is intricately sheared. Study of the oriented returned samples shows that movement along some of the shear planes has deformed clasts. In addition, at least one shear set apparently occurs only within the blue-gray breccia portion of the boulder.

Major events recorded in the station 6 boulder are the formation of the parent of the light gray breccia, its brecciation and incorporation as inclusions in the blue-gray breccia, and subsequent enclosure of the blue-gray breccia in the greenish-gray breccia as shown by the occurrence in the latter of blue-gray breccia clasts. Local brecciation of the blue-gray breccia and its inclusions produced light gray breccias with clasts of blue-gray breccia.

The station 7 boulder is similar to the station 6 boulder in that the two major rock types, greenish-gray and blue-gray breccia, are present. The contact between the two types is a sharp,

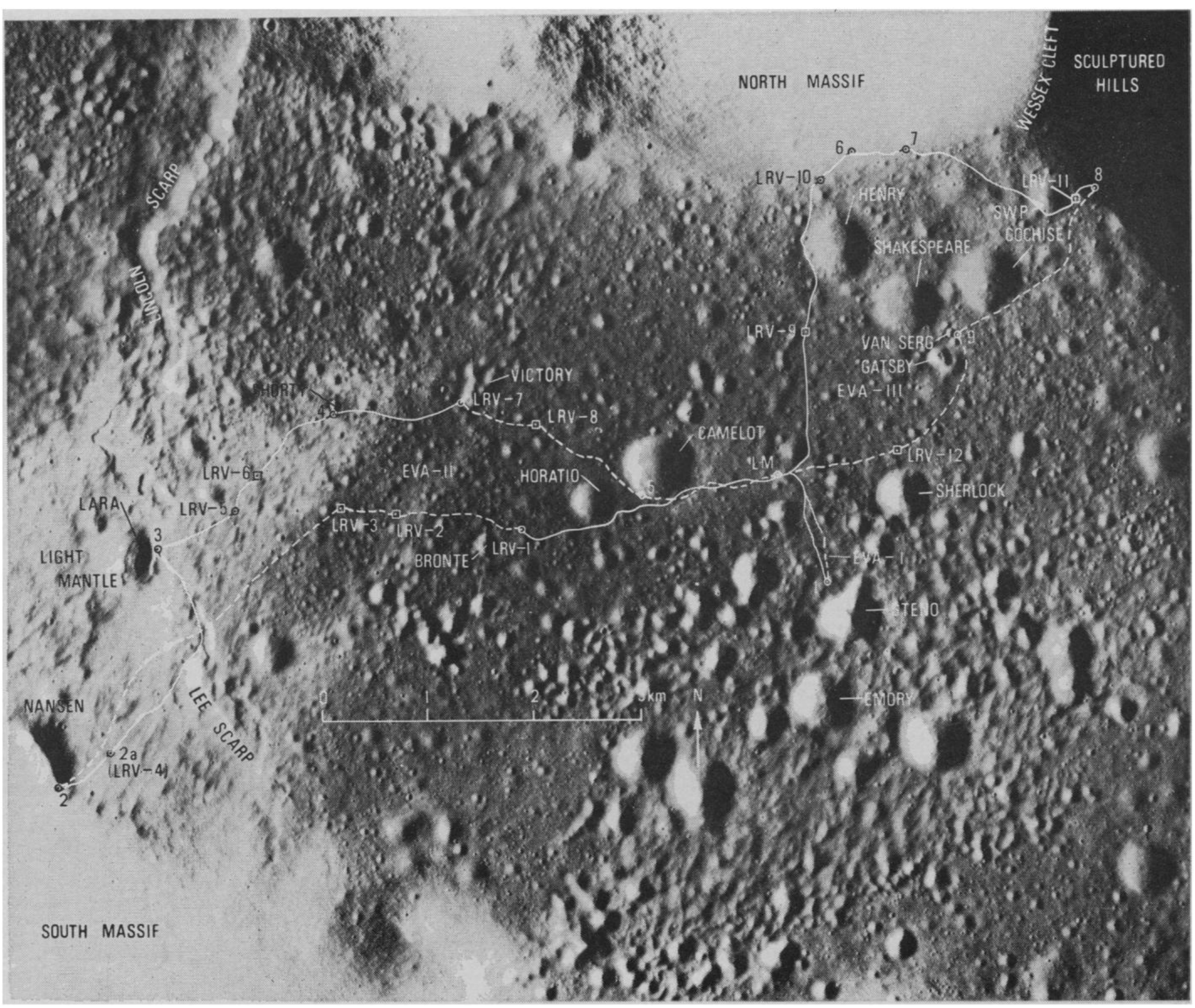

Fig. 2. Index map of the traverse area showing stations (LM and 1 to 9) and Lunar Rover sample stops (LRV-1 to LRV-12); (circles) locations accurate within 10 m; (squares) approximate locations; (solid line) traverse path, derived in part from very-long-baseline interferometry by I. Salzburg, Goddard Space Flight Center; (dashed line) approximate traverse. [NASA panoramic camera photograph 2309]

irregular boundary. The greenish-gray material appears to enclose the blue-gray breccia.

A large (1.5 by 0.5 m) white clast similar to those in the station 6 boulder is penetrated by narrow blue-gray breccia dikes in the station 7 boulder (Fig. 7). The clast consists of friable white cataclasite that is cut by an irregular network of dark gray, fine-grained veins. The vein-cataclasite complex was weakly brecciated to isolate some small pieces of the vein in the white matrix. Other irregular thin blue-gray veinlets branch from the main dike into the white cataclasite.

The station 7 boulder is intricately fractured. At least two fracture sets that are well developed in the large white clast and its dikes, as well as in the blue-gray breccia host, are not seen in the greenish-gray breccia. This suggests that the fracturing occurred in the blue-gray breccia before its incorporation in the greenish-gray breccia. Additional evidence for the younger age of the latter is that the foliation of the vesicles in it is parallel to the contact with the blue-gray breccia. As in the station 6 boulder, the youngest event is represented by the greenish-gray breccia, and the oldest by the large white clast in the blue-gray breccia.

South Massif boulders most probably came from the highest part of the massif, and the boulders from stations 6 and 7 probably came from within the lower one-third of North Massif. Hence two different stratigraphic intervals could have been sampled. On the other hand, the lithologies of the South Massif boulders resemble those of the North Massif boulders in many respects. The greenish-gray breccia and blue-gray breccia, seen as discrete boulders at station 2, are components of the boulders at stations 6 and 7, which suggests that these breccias may represent a single stratigraphic unit. Whether from one or more stratigraphic units, the massif samples consist of complex breccias reasonably interpreted as ejecta from ancient large impact basins.

Fine-grained regolith is ubiquitous on the part of the sculptured hills visible at station 8 (Fig. 2), and no boulders that clearly represent the bedrock of the hills were found. The lack of blocks around fresh craters up to 50 m in diameter indicates that bedrock is more than 10 m below the surface slope material. The soil in this area, at least to the depth of the trench samples, 20 to 25 cm, consists of fine-grained, cohesive clods and particles.

Small fragments of basalt, probably ejected from craters on the valley floor, and regolith breccia dominate the samples, which consist mainly of chips

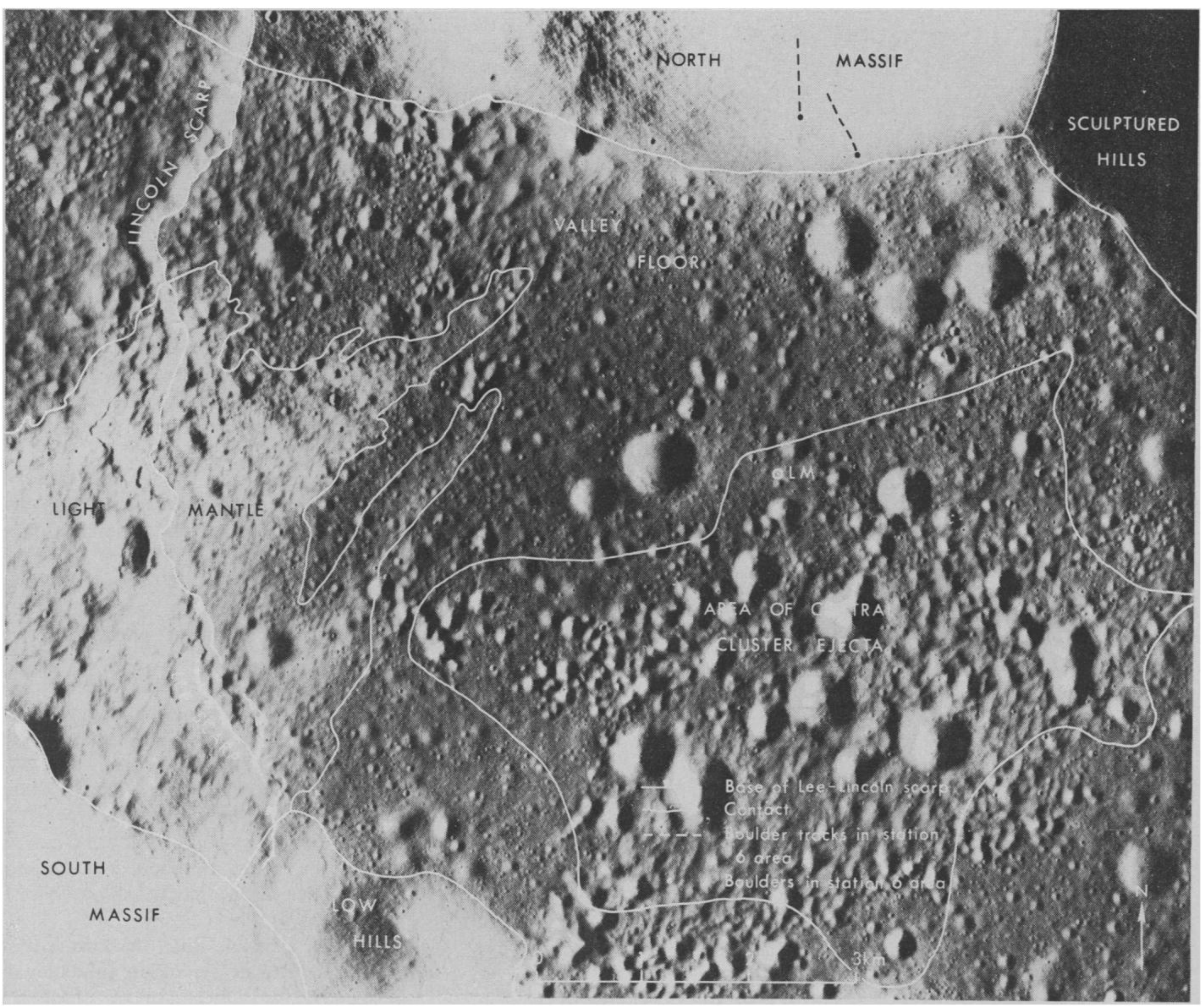

Fig. 3. Generalized geologic map of the Apollo 17 traverse area. Boulders indicated only at station 6. [NASA panoramic camera photograph 2309]

collected with soils or by raking. Samples of friable feldspathic breccia from the wall of a 15-m crater and of a glass-covered gabbroic boulder, both of which are almost certainly exotic, were also collected. The greater dissection, lower slopes, lack of large boulders, and limited sample suite suggest that the sculptured hills may be underlain by less coherent rocks than the massifs.

Subfloor Basalt

Subsequent to the formation of the Taurus-Littrow graben by the Serenitatis impact, the valley floor was inundated and leveled by basaltic lava flows. Geophysical evidence (*8, 9*) suggests that the prism of basalt filling the valley is more than a kilometer thick. Apparently the uppermost 130 m of this so-called subfloor basalt was sampled in the dark portions of the valley floor, where it occurs both as scattered blocks and fragments and as concentrations of blocks on the walls and rims of the larger craters. The areas in which the basalts were most thoroughly sampled were on the rims of Shorty and Camelot craters (stations 4 and 5), in the central cluster ejecta (LM area), and on the ejecta blanket of Steno Crater (station 1).

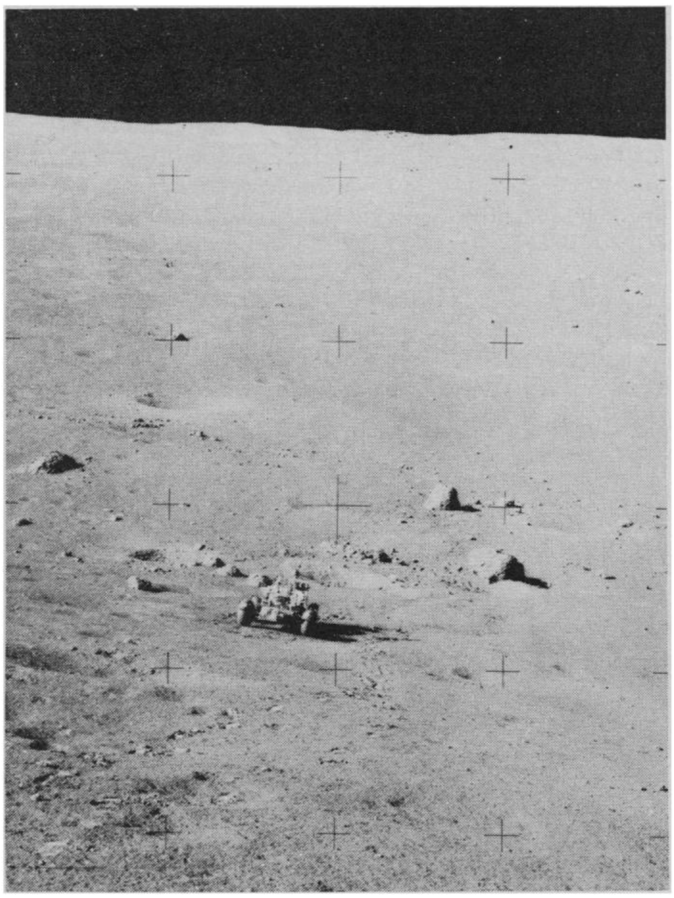

Fig. 4. Part of South Massif showing area sampled at station 2 at the Apollo 17 landing site. The two large boulders upslope and to the right of the Rover and the small boulder immediately above the edge of the umbrella-like antenna were studied and sampled. The blocky area on the skyline, approximately 1400 m above the Rover, is the probable source of the station 2 boulders. Boulder tracks, not visible in this photograph, originate near the blocky area. [NASA photograph AS17-138-21072]

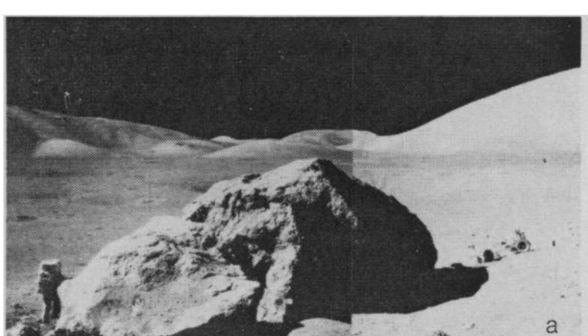

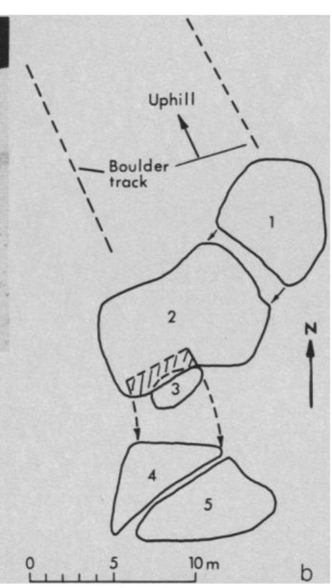

Fig. 5. (a) Station 6 boulder, showing fragments 1 and 2 of the five that comprise the broken boulder. The view is to the south. [NASA photographs AS17-140-21494, 21497] (b) Map of station 6 boulder showing relationships of large fragments and their most probable reassembly.

In general the subfloor basalt blocks seen at the landing site were not visibly shocked or even intensely fractured. The most notable exception was an intensely fractured 5-m boulder on the rim of Shorty Crater. The predominant types described on the lunar surface were coarse-grained, vesicular, relatively light-colored basalts composed of clinopyroxene, ilmenite, and 30 to 40 percent plagioclase. Vesicles up to about 1 cm in diameter typically comprised 10 to 15 percent of these rocks. In some rocks, planar partings are parallel to planar concentrations of vesicles. Fine-grained and less vesicular varieties of basalt were recognized locally.

Returned samples of basalt may be grouped in hand specimens into five classes: (i) vesicular, porphyritic, coarse-grained basalts; (ii) vesicular, coarse-grained basalts; (iii) vesicular, fine-grained basalts; (iv) dense aphanitic basalts; and (v) vesicular aphanitic basalts. Individual samples of the first two of these types were generally termed vesicular gabbro by the Apollo 17 crew. Examples of the last three were described as fine-grained basalt, basalt, and obsidian, respectively.

In general the basalts are holocrystalline and rich in ilmenite (more than 15 percent), which commonly lines vugs and vesicles. Olivine occurs in trace amounts in all types. Pyroxene occurs as composite phenocrysts enclosing ilmenite in the porphyritic type. Plagioclase poikilitically encloses pyroxene and ilmenite in the coarse-grained types. Groundmass grain size ranges from about 0.1 mm in the aphanitic basalts to about 1.5 mm in the coarse-grained types. The pyroxene-ilmenite intergrowths that form the phenocrysts of the porphyritic coarse-grained basalts are about 3 to 4 mm in diameter and comprise about 5 to 15 percent of the rock.

It is possible that the two coarse-grained basalt types are gradationally related by a decrease of porphyritic pyroxene-ilmenite aggregates, but our best judgment at present is that they

Fig. 6. Driving photos taken between the LM and station 6. Note the light color of "turning point" rock and the station 6 boulders, in contrast to the dark color of the large boulder farther up the slope. The dark boulder originated from higher on the massif (500 m below the summit) than the lighter colored station 6 boulder (1000 m below the summit), suggesting that darker rocks might overlie light rocks in the North Massif. [NASA photographs AS17-141-21549, 21550]

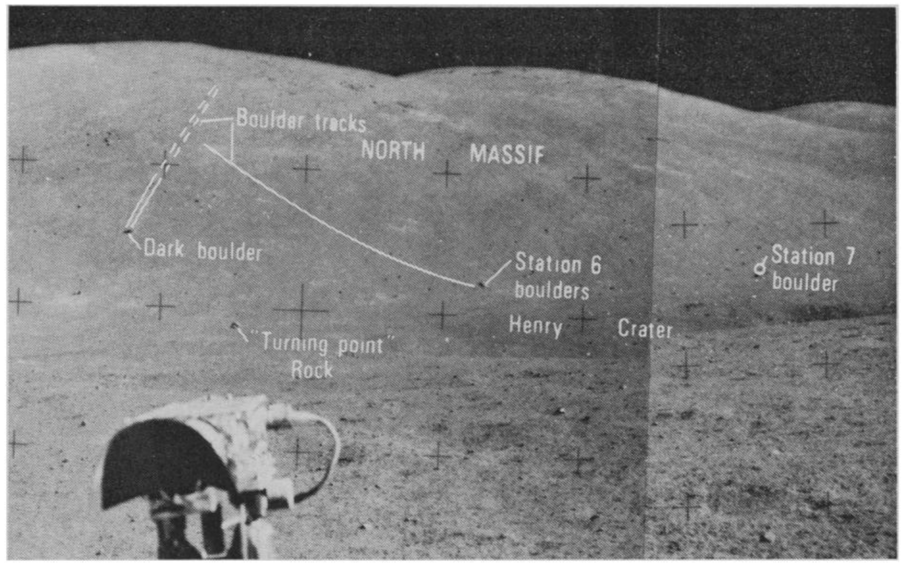

represent separate flow units. It seems likely that the vesicular fine-grained basalts are gradationally related to the vesicular aphanitic basalts through a decrease in grain size and an increase in vesicle size. The dense aphanitic basalts seem to be fragments of a separate flow unit.

Sampled subfloor basalts were most probably derived from depths between about 20 and 130 m. The stratigraphically lowest basalt unit is interpreted as the vesicular coarse-grained basalt sampled at the rim of Camelot Crater. This unit may be overlain by the coarse-grained porphyritic type sampled in the LM area. The next stratigraphic unit, proceeding upward, is the vesicular fine-grained basalt represented in the Steno ejecta, and the aphanitic basalts of the Shorty ejecta may be the shallowest recognizable types. It should be stressed that this stratigraphic succession, which is based on inferred depth of evacuation and on textural features, is speculative.

Radiometric age determinations (*10, 11*) suggest that filling of the valley by lava flows may have been completed by about 3.8×10^9 years ago. Before the final accumulation of mare fill to the west in the Serenitatis basin, broad arching just east of the basin tilted the subfloor lavas to the east, as shown in the present 1° eastward tilt of the valley floor.

Surficial Materials

The dominant surficial deposits of the highlands are the thick talus deposits that form continuous aprons on the lower slopes and the impact-generated regolith. The upper slopes of the massifs are nearly free of regolith as is shown by exposures of bouldery zones that may represent near-surface bedrock. At stations 2, 6, and LRV-10 (Fig. 2), located on the gentle slopes immediately above the valley floor, fillets occur preferentially on the upslope sides of boulders. This indicates that debris is currently moving down the slopes.

Along much of the base of South Massif the talus intersects the valley floor at a sharp angle, which suggests that downslope movements have been active so recently, perhaps as a consequence of recent massif uplift, that impact processes have not had time to round the knickpoint. Part of this talus deposit has filled about three-quarters of Nansen Crater. The present appearance of the massif slope into Nansen is that

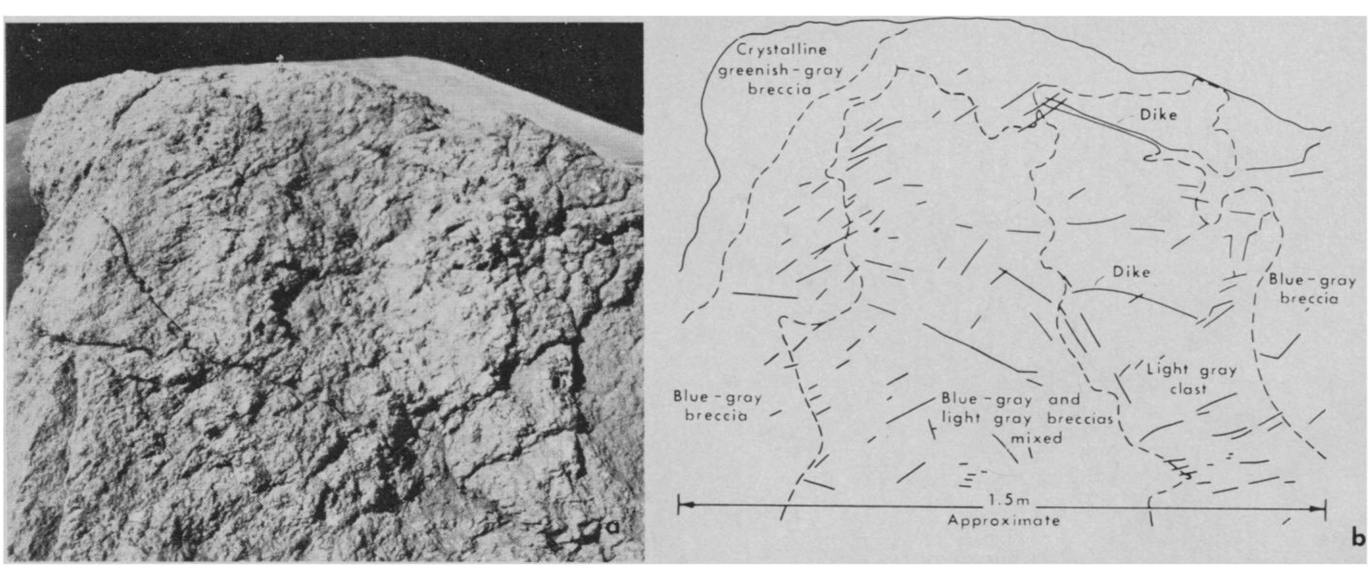

Fig. 7. (a) Station 7 boulder. Dikes of blue-gray breccia in light gray clast within blue-gray breccia. [NASA photograph AS17-146-22305] (b) Sketch map of station 7 boulder. Except for labeled dikes and the outline of the boulder, solid lines indicate traces of fractures.

of an active talus apron that is slowly continuing to fill the crater.

Formation of talus deposits as well as mass movements of highlands materials onto the valley floor should date back to the earliest uplift of the massifs. If the bounding faults were, as we suppose, steeper than the angle of repose for loose fragments, there must have been a large transfer of material down the newly formed slopes until the angle of repose was reached. Thus it is inferred that deposits from mass movements and thick talus aprons buried by subfloor basalt overlie the still older rocks that formed the initial floor and walls of the Taurus-Littrow valley.

Fragmental surficial materials of the valley floor, where cut by Shorty and Van Serg craters, are of the order of 15 m thick. Part is undoubtedly impact-generated regolith similar to that developed on mare basalts elsewhere on the moon. Other components of the surficial deposits of the valley are the central cluster ejecta, the light mantle, and perhaps the elusive dark mantle.

The ejecta of 90-m Van Serg Crater includes a large proportion of soft, dark, matrix-rich breccias interpreted as soil breccias derived from the lower part of the valley floor regolith. The breccias are dark to very dark gray, friable, and have numerous penetrative fractures. The surfaces of the penetrative fractures are weakly slickensided as was typical of regolith breccias returned by earlier Apollo missions. Clasts larger than 1 mm make up from 1 to about 15 percent of the breccias; most clasts are smaller than 1 cm. However, on the rim of Van Serg Crater, scattered light gray lithic clasts range up to about 2 cm in diameter, and in the fragment-rich breccia of the crater floor, which has a dark matrix, the crew saw light clasts up to ½ m in diameter. Some of the breccia is layered, with alternating layers of the order of several centimeters thick that are distinguished by differing clast abundances.

The Van Serg breccias probably represent regolith materials indurated by the impact that formed Van Serg Crater. As far as we know, subfloor basalt was not excavated by the impact, although traverse gravity data (*8*) imply its presence in the subsurface. At least 15 m of regolith material is thought to have overlain the subfloor basalt in the Van Serg area when the crater was formed. The deepest part, represented by the rocks of the Van Serg rim and floor, is considered older than the central cluster ejecta, and hence represents older regolith material.

The complex ejecta blanket of the cluster of large craters south and east of the LM (Fig. 3) is distinguished by an abundance of blocks visible at the surface. Younger deposits are apparently too thin to fully bury the blocks in the unit, and the unit is too young for the blocks to have been reduced much in size by later impacts. Fine-grained ejecta probably extend discontinuously beyond the area in which blocks can be seen and may be present at such places as station 5. The deep core, obtained about 200 m west of the LM and more than a crater diameter from any large crater of the cluster, may have penetrated the entire unit. The change of soil appearance (*12*), seen in core-stem joints, at a depth of about 1 m may coincide with the base of the central cluster ejecta.

Deposition of the central cluster ejecta created an immature basalt-rich regolith surface layer overlying more mature regolith like that of the Van Serg soil breccias. The immaturity of the surface layer is most easily seen in the common occurrence of blocks and rock fragments. It is also reflected by the preponderance of subfloor basalt fragments and scarcity of exotic components such as ejecta from impacts in the highlands.

The young pyroclastic dark mantle that was anticipated before the mission was not recognized in the traverse area as a discrete surface layer. Strong photogeologic evidence of such a mantle on the valley floor and in parts of the highlands still exists and is summarized by Lucchitta (*13*):

1) The dark mantle covers older, dark mare material on a bench at the southeastern edge of the Serenitatis basin and may extend beyond onto the younger Serenitatis mare fill.

2) In the nearby mountains the dark deposit mantles depressions between hills and also occurs as patches or streaks on steep slopes.

3) The dark mantle drapes over and subdues the underlying topography.

4) The dark mantle usually appears smooth and velvety with no blocks visi-

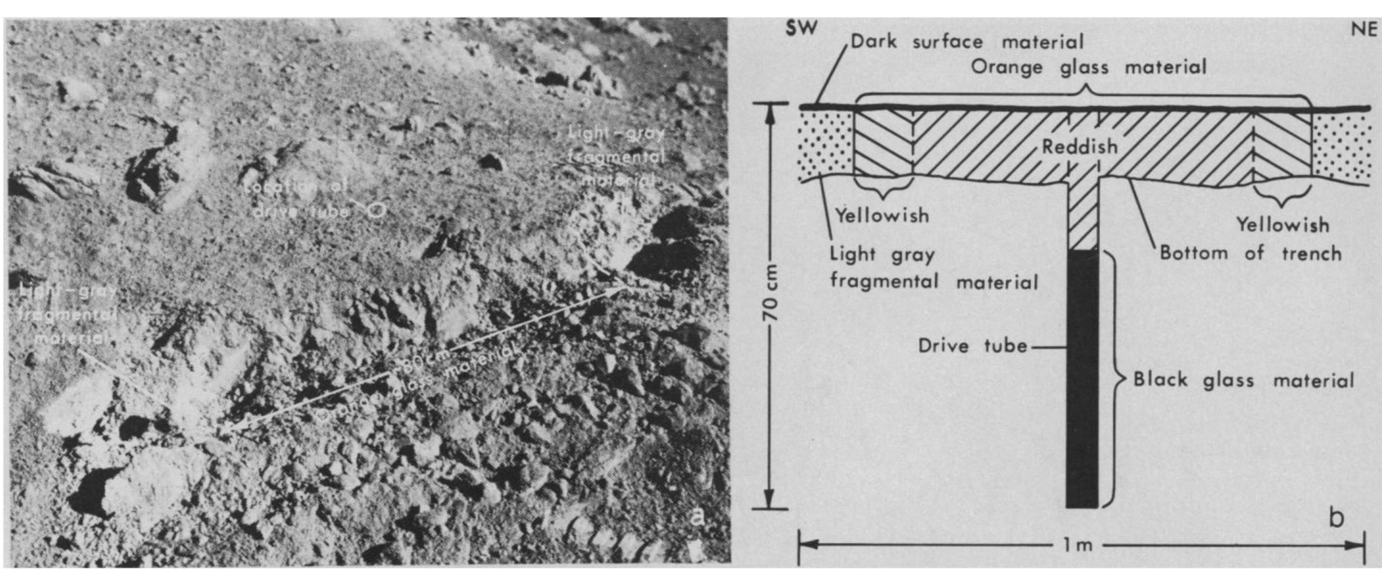

Fig. 8. (a) North-looking photograph showing orange glass material and light gray fragmental material exposed in trench on rim crest of Shorty Crater. [NASA photograph AS17-137-20986] (b) Cross section showing materials in trench and double drive tube of Shorty Crater rim crest.

ble in photographs with a resolution of 2 m.

5) Darker areas in the lowlands seem to be associated with a higher degree of smoothing of craters.

6) The dark material overlies massifs and Imbrian mare, and it covers Imbrian grabens and fresh-looking scarps and mare ridges. It may mantle craters as young as middle Copernican in age and is overlain only by deposits of very young craters (late Copernican) and by the light mantle.

Albedo measurements made from orbital photographs show that the eastern part of the valley floor and small depressions with dark floors in the highlands are much darker relative to the underlying bedrock than is normal for lunar regolith. The abnormal surface darkening strongly suggests that exotic dark material has been introduced to the Taurus-Littrow area.

The weight of evidence favors the formation of a dark mantle some time after extrusion of the subfloor basalt in the Taurus-Littrow region. Although no discrete dark mantle layer was recognized, tiny opaque black spheres that may cause the low albedo are abundant in the soil samples (*12*). If the dark material was deposited later than central cluster ejecta, it must be so thin in the landing site that it is thoroughly intermixed with the younger part of the regolith. An alternative hypothesis is that the dark mantle material may have accumulated shortly after the extrusion of the subfloor basalt. This is suggested by the age of 3.71×10^9 years for the orange glass spheres (*11*) which are associated with black glass spheres on the rim of Shorty. In this case the deposit would be intimately mixed throughout the subsequently formed regolith.

The light mantle is an unusual deposit of high-albedo material with fingerlike projections that extends 6 km across the dark plains from South Massif (Fig. 3). In the absence of an impact crater from which it might have been a ray of ejecta, the light mantle was interpreted from pre-mission photographs as a probable landslide or avalanche from the steep northern slope of South Massif (*2, 4, 14*). The materials collected at stations 2, 2a, and 3 on the light mantle are similar to those that comprise South Massif, which supports this hypothesis.

The light mantle is mainly unconsolidated fines in which rocks larger than 25 cm across are scarce. The avalanche apparently consisted mainly of regolith from the surface of the massif and did not involve sliding of underlying bedrock.

The size-frequency distribution and morphologies of craters on the light mantle suggest that its age is about that of the crater Tycho, or of the order of 100×10^6 years. Crater counts show that the saturation crater size is 2 to 4 m. The saturation crater size at Tycho is 2.8 m (*15*).

The light mantle is larger is areal extent than most other lunar avalanches and, unlike many, has no conspicuous source ledge on the slope above. A cluster of 100-m craters occurs on the top of South Massif, and a similar cluster occurs on the plains adjacent to the northwest side of the light mantle (*5*). The clustered craters appear to be secondaries from a distant crater to the south, such as Tycho. Impacts on the northwest slope of South Massif from the same swarm of projectiles that formed the clustered craters could have initiated the avalanche. Elsewhere on the moon, other avalanches are known to have been triggered by the impacts of secondary projectile swarms on slopes facing away from the primary crater (*14*).

Fine-grained soil, darker than the underlying unconsolidated debris, was recognized at the surface at Shorty, Van Serg, on the light mantle, and on the massif talus. It is thin—½ cm at Shorty and about 7 cm on the flank of Van Serg. It probably represents the regolith that has formed on these relatively young surfaces.

Shorty Crater—Orange Soil

Shorty Crater, a fresh impact crater 110 m in diameter penetrating the northern part of the light mantle, is of special interest because of the exposures of orange soil in its rim and wall. Its blocky floor may represent either impact-indurated soil breccia or the top of the subfloor basalt, which is buried by 10 to 15 m of poorly consolidated regolith, including light mantle. The predominantly fine-grained wall, rim, and flank materials are probably ejecta derived largely from materials above the subfloor, and the basalt blocks at station 4 may be ejecta derived from the subfloor.

Unusual concentrations of orange soil are known to occur in two places on the crest of the crater rim as well as in the ejecta of a small, fresh crater high on the northwest interior wall. A trench exposed an orange zone 80 cm wide (Fig. 8) that trends parallel to the crest for several meters. The orange soil is markedly coherent as shown by systematic fractures in the trench wall. It is also zoned; a wide central reddish zone, now known to consist largely of small red and orange glass spheres and fragments, grades laterally to marginal yellowish zones about 10 cm wide (Fig. 8). The yellowish zones in turn are in sharp steep contact with light-gray fragmental material that is probably typical of the crater rim. A double drive tube placed in the axial portion of the colored zone bottomed in black fine-grained material now known to consist of tiny, opaque, black spheres. The contact between orange and black glass occurs within the upper drive tube at a depth estimated from the debris smeared on the exterior of the tube to be about 25 cm.

The origin of the red and black glass materials is uncertain. A radiometric age determination of 3.71×10^9 years for the orange glass material (*11*) implies solidification during or shortly after the period of subfloor basalt volcanism. Shorty Crater, of course, is much younger. Such glass, whether ejected from an impact crater or a volcanic vent, may have lain as a layer (or layers) either within the upper part of the subfloor basalt sequence or deep within the regolith overlying the subfloor basalt in the target area. If so, the orange and black glassy materials may represent clods of ejecta excavated by the Shorty impact. However, the symmetrical color zonation of the orange soil and apparent parallelism of the zone's steep boundaries with both the internal color banding and the axis of the rim crest are improbable features for a clod of ejecta unless the clod underwent alteration after its emplacement, a process heretofore unknown on the moon. The color zoning and steep contacts might be more readily explained if the glass material, derived from a layer of similar material in the target, were mobilized by the impact and driven dike-like into concentric fractures. However, the occurrence of black glass material below the orange glass material in the double drive tube (Fig. 8) and the absence of the black glass at the surface suggest the existence of horizontal or gently dipping layering, a geometric arrangement that would be reasonable in a clod of ejecta but is difficult to reconcile with injection of old glass material into a concentric fracture.

The possibly younger age (*10, 11*) and distinctly more ultrabasic composition (*16*) of the orange glass suggest that its origin may be separate from that of the subfloor basalt. Three sequences of mare basalt have been discriminated near the Apollo 17 landing site (*17*). The oldest includes the subfloor basalt of the Taurus-Littrow valley; the youngest is the main fill of Mare Serenitatis, which generally seems free of dark mantling materials. We propose that the orange glass and dark mantle are related to the intermediate stage of basalt volcanism, which, along with the oldest (subfloor) basalt sequence, may represent Tranquillitatis mare fill.

Structural Geology

The Taurus-Littrow valley is bounded by high steep-sided mountain blocks that form part of the mountainous southeastern rim of the Serenitatis basin. Each massif block is probably a structural unit uplifted during the Serenitatis event along high-angle faults that are largely radial and concentric to the Serenitatis basin.

Rejuvenation of these older structural elements of the Taurus-Littrow valley, which is radial to both Imbrium and Serenitatis, could have occurred during the Imbrium event (*3, 4*). Segmentation of the massifs may be an inheritance from the even earlier Tranquillitatis event.

The massifs adjacent to the landing site appear similar in slope, albedo, and degree of cratering. They are unlike the closely spaced domical sculptured hills, which also form fault block mountains (*3*). No unequivocal sculptured hills material has been recognized among the samples; hence the reason for the differing appearance of the massifs and the sculptured hills is not understood.

Single, major bounding faults are inferred along the face of each mountain block. Such faults can be recognized at the margins of younger, less modified basins (such as Orientale and Imbrium). These faults are probably very steep—more than 60° and probably close to 90° for the radial faults. They are buried under the talus aprons and lie valleyward from the lowest outcrops visible on the massif faces. Sharp knickpoints at the massif bases suggest that additional later uplift may have reinitiated downslope movement of talus.

The Taurus-Littrow valley appears to be a long, narrow graben radial to the Serenitatis basin. The present uniformity of the valley floor is due to the continuity of the valley fill surface. The fill probably consists of rubble that was created at the time of block faulting, and is overlain by subfloor basalt and still later regolith material that are younger than any large differential movements of the structural blocks.

The valley floor slopes about 1° toward its eastern end. This small dip is interpreted as structural rather than depositional because it occurs within an east-tilted belt that also includes the floor of the crater Littrow (Fig. 1). The tilt is interpreted as recording the development of a broad arch formed by uplift along the mountainous Serenitatis rim after the subfloor basalt fill had accumulated in the Taurus-Littrow graben. Long, shallow grabens largely concentric to the Serenitatis basin were created during this deformation. They were truncated by younger mare filling deposits that subsequently accumulated in the Serenitatis basin (*17*).

Younger deformational features on the valley floor include the Lee-Lincoln scarp and several small, sharp grooves that are visible on the surface of the light mantle in the photographs taken at a low sun angle with the Apollo 17 panoramic camera. The grooves appear to be small grabens similar to the small graben rilles that are common on mare surfaces. They were probably formed by minor tectonic movements that occurred after the emplacement of the light mantle.

The Lee-Lincoln scarp is characterized by a steep face that generally faces east, commonly in a pair of steps whose total relief reaches 80 m in the center of the valley. A few prominent smaller scarps face west. Individual segments die out along the strike as others pick up the displacement; in places the scarp appears almost braided. The trends of individual segments of the scarp appear to alternate between north and northwest as if controlled by an underlying prismatic fracture system. This same set of trends is identifiable in segments of the scarp along the west base of North Massif. Here the single scarp faces east toward the massif, in the form of a reverse or thrust fault. Forty kilometers to the north the scarp passes out onto the dark plains surface where it cuts Rima Littrow I (Fig. 1).

The overall length, trend, asymmetry, and morphologic character of the scarp resemble those of the larger wrinkle ridges of the adjacent Serenitatis mare. This suggests a common origin—possibly folding and thrusting of a thin plate (decollement sheet) eastward (*18*). The relative youth of this deformation is indicated by the transection of fresh Copernican craters by wrinkle ridges in the mare; by the fresh, possibly rejuvenated scarplets that may be younger than the light mantle; and by the good preservation of the scarp in the unconsolidated materials of the face of North Massif. An alternative possibility is that the Lee-Lincoln scarp is the surface trace of a complex high-angle fault that changes strike where it follows the old North Massif boundary fault immediately north of the valley.

References and Notes

1. P. M. Muller and W. L. Sjogren, *Science* **161**, 680 (1968).
2. E. W. Wolfe, V. L. Freeman, W. R. Muehlberger, J. W. Head, H. H. Schmitt, J. R. Sevier, *Geotimes* **17** (No. 11), 14 (1972).
3. J. W. Head, *Moon*, in press.
4. D. H. Scott, B. K. Lucchitta, M. H. Carr, in *Geologic Atlas of the Moon* (Map I-800, U.S. Geological Survey, Washington, D.C., 1972).
5. B. K. Lucchitta, in *ibid.*, sheet 2.
6. Correlation of rock names used in this article with field names [H. H. Schmitt, *Science* **182**, 681 (1973)] is given by the Apollo Field Geology Investigation Team, in (*7*).
7. *Apollo 17 Preliminary Science Report* (National Aeronautics and Space Administration, Washington, D.C., in press).
8. M. Talwani, G. Thompson, B. Dent, H-G. Kahle, S. Buck, in (*7*).
9. R. L. Kovach, J. S. Watkins, P. Talwani in (*7*).
10. Eight age determinations on six basalt fragments from the valley floor gave values ranging from approximately $(3.71 \pm 0.07) \times 10^9$ years to $(3.83 \pm 0.10) \times 10^9$ years. The mean of these isotopic ages is 3.78×10^9 years. N. M. Evensen, V. R. Murthy, M. R. Coscio, Jr., *Trans. Amer. Geophys. Union* **54**, 581 (1973); T. Kirsten, P. Horn, D. Heymann, W. Hübner, D. Storzer, *ibid.*, p. 595; M. Tatsumoto, P. D. Nunes, R. J. Knight, C. E. Hedge, D. M. Unruh, *ibid.*, p. 614; L. Husain and O. A. Schaeffer (*11*); F. Tera, D. A. Papanastassiou, G. J. Wasserburg, report presented at the Fourth Lunar Science Conference, Houston, Texas (1973).
11. L. Husain and O. A. Schaeffer, *Science* **180**, 1358 (1973).
12. Lunar Sample Preliminary Examination Team, in (*7*).
13. B. K. Lucchitta, in (*7*).
14. K. A. Howard, *Science* **180**, 1052 (1973).
15. E. C. Morris and E. M. Shoemaker, in *Surveyor Project Final Report. Part 2: Science Results, Tech. Rep. 32-1265* (Jet Propulsion Laboratory, Pasadena, 1968), p. 65.
16. J. M. Rhodes, K. V. Rogers, B. Bansal, in *Lunar Sample Information Catalog, Apollo 17* (Lunar Receiving Laboratory, Lyndon B. Johnson Space Center, Houston, 1973), p. 50.
17. K. A. Howard, M. H. Carr, W. R. Muehlberger, in (*7*).
18. K. A. Howard and W. R. Muehlberger, in (*7*).

19. Work done under NASA contract T-5874A. Publication authorized by the director, U.S. Geological Survey.